

Effect of the Leaving Ligand X on Transmetalation of Organostannanes (vinylSnR₃) with L_nPd(Ar)(X) in Stille Cross-Coupling Reactions. A Density Functional Theory Study

Alireza Ariafard,^{*,†} Zhenyang Lin,^{*,‡} and Ian J. S. Fairlamb[§]

Department of Chemistry, Faculty of Science, Central Tehran Branch, Islamic Azad University, Felestin Square, Tehran, Iran, Department of Chemistry, The Hong Kong University of Science and Technology, Clear Water Bay, Kowloon, Hong Kong, and Department of Chemistry, University of York, Heslington, York, YO10 5DD, U.K.

Received August 23, 2006

Density functional theory calculations were carried out to study the effect of different leaving ligands X on transmetalation of organostannanes (vinylSnR₃) with L_nPd(Ar)(X) (X = Cl, Br, I), an important step found in Stille cross-coupling processes. The calculations indicate that the overall activation barriers for the transmetalation process increase in the following order: X = Cl < Br < I. The model phosphine ligands, PH₃ and PMe₃, were used to investigate this process. It was established that more electron-donating phosphine ligands significantly increase the overall transmetalation barriers.

Introduction

The formation of new C–C bonds through cross-coupling reactions catalyzed by palladium has received considerable interest in recent years due to their importance in many synthetic applications.^{1,2} Pd-catalyzed cross-couplings of organic electrophiles (RX) with organostannanes (vinylSnR'₃), better known as Stille reactions, are widely used, particularly in more demanding synthetic transformations, e.g., in natural product or materials synthesis.^{3,4} The popularity associated with this reaction stems from the fact that the organostannane reagents

tolerate a variety of functional groups, which are stable to both moisture and oxygen.

The commonly accepted catalytic cycle for the mechanism of Stille cross-coupling reactions of organic halides with organostannanes is shown in Scheme 1.⁵ The first step of the catalytic cycle involves oxidative addition of an organic halide (RX) to the active species L_nPd⁰ (n = 1, 2), which is usually generated from a L₂Pd^{II}X₂ precatalyst, where L is typically a phosphine ligand and X is halide. The organopalladium(II) species L_nPd(R)(X) formed by the oxidative addition of the organic halide then undergoes transmetalation with organostannanes (R'SnR''₃) to afford L_nPd(R)(R'). Finally, a reductive elimination reaction occurs in L_nPd(R)(R'), leading to C–C bond formation (R–R').

The mechanism of Stille cross-coupling has been well studied both experimentally⁶ and theoretically.^{7,8} Specifically, the thorough mechanistic studies by Espinet and co-workers established the primary importance of a S_E2(cyclic) mechanism for the transmetalation step for X = halide (Scheme 1).⁶ A recent DFT study provided support for such an S_E2(cyclic) mechanism.⁸

During the course of these mechanistic studies, Espinet and co-workers found that the transmetalation reactions of (vinyl)SnBu₃ with isolated *trans*-[Pd(Ar)(X)(AsPh₃)₂] (Ar = 3,5-dichlorotrifluorophenyl; X = halide) exhibit rates of Cl > Br > I.^{6a} This trend was explained as follows. First, an electronegative leaving ligand makes the Pd(II) metal center more electrophilic, facilitating the nucleophilic attack of R'SnR''₃ on the Pd(II) complex.^{6a} It was also noted that aryl iodides undergo oxidative addition more rapidly than aryl bromides, although crucially the rate-determining transmetalation of the resulting

* Corresponding authors. E-mail: ariafard@yahoo.com; chzlin@ust.hk.

† Islamic Azad University.

‡ The Hong Kong University of Science and Technology.

§ University of York.

(1) (a) Miyaura, N.; Suzuki, A. *Chem. Rev.* **1995**, *95*, 2457. (b) Meijere, A. De; Meyer, F. E. *Angew. Chem., Int. Ed.* **1995**, *33*, 2379. (c) Ishiyama, T.; Miyaura, N. *J. Organomet. Chem.* **2000**, *611*, 392. (d) Beletskaya, I. P.; Cheprakov, A. V. *Chem. Rev.* **2000**, *100*, 3009. (e) Wolfe, J. P.; Tomori, H.; Sadighi, J. P.; Yin, J.; Buchwald, S. L. *J. Org. Chem.* **2000**, *65*, 1158. (f) Ehrentraut, A.; Zapf, A.; Beller, M. *Adv. Synth. Catal.* **2002**, *344*, 209. (g) Miyaura, N. *Top. Curr. Chem.* **2002**, *219*, 11. (h) Tamao, K.; Hiyama, T.; Negishi, E. *J. Organomet. Chem.* **2002**, *653*, 1. (i) Cárdenas, D. *J. Angew. Chem., Int. Ed.* **2003**, *42*, 384. (j) Cárdenas, D. *J. Angew. Chem., Int. Ed.* **2003**, *42*, 384. (k) For a special issue dedicated to the development and application of highly active and selective palladium catalysts, see: Fairlamb, I. J. S. *Tetrahedron* **2005**, *61*, 9661 (symposium-in-print 113).

(2) (a) Sumimoto, M.; Iwane, N.; Takahama, T.; Sakaki, S. *J. Am. Chem. Soc.* **2004**, *126*, 10457. (b) Braga, A. A. C.; Morgon, N. H.; Ujaque, G.; Maseras, F. *J. Am. Chem. Soc.* **2005**, *127*, 9298. (c) Goossen, L. J.; Koley, D.; Hermann, H. L.; Thiel, W. *J. Am. Chem. Soc.* **2005**, *127*, 11102.

(3) (a) Milstein, D.; Stille, J. K. *J. Am. Chem. Soc.* **1978**, *100*, 363. (b) Stille, J. K. *Angew. Chem., Int. Ed. Engl.* **1986**, *25*, 508. For applications in natural product synthesis of our research, see: (c) Burling, S.; Crawford, C. M.; Fairlamb, I. J. S.; Kapdi, A. R.; Taylor, R. J. K.; Whitwood, A. C. *Tetrahedron* **2005**, *61*, 9736. (d) Demotie, A.; Fairlamb, I. J. S.; Lu, F.-J.; Shaw, N. J.; Spencer, P. A.; Southgate, J. *Bioorg. Med. Chem. Lett.* **2004**, *14*, 2883. (e) Crawford, C. M.; Fairlamb, I. J. S.; Taylor, R. J. K. *Tetrahedron Lett.* **2004**, *45*, 461. (f) Crawford, C. M.; Burling, S.; Fairlamb, I. J. S.; Taylor, R. J. K.; Whitwood, A. C. *Chem. Commun.* **2003**, 2194.

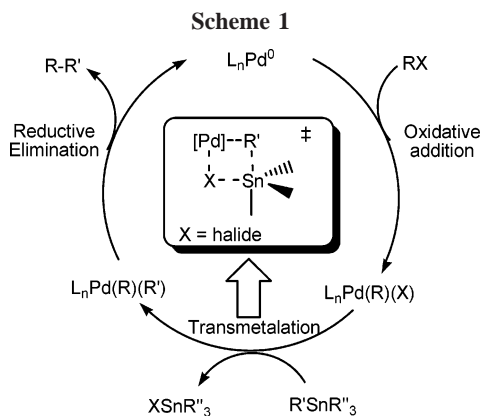
(4) (a) Farina, V. In *Comprehensive Organometallic Chemistry II*; Abel, E. W., Stone, F. G. A., Wilkinson, G., Eds.; Pergamon: Oxford, 1995; Vol. 12. (b) Mitchell, T. N. In *Metal-catalyzed Cross-coupling Reactions*; Diederich, F., Stang, P. J., Eds.; Wiley-VCH: New York, 1998. (c) Kosugi, M.; Fugami, K. In *Handbook of Organopalladium Chemistry for Organic Synthesis*; Negishi, E., Ed.; Wiley: New York, 2002. (d) Tsuji, J. *Palladium Reagents and Catalysts*; Wiley: Chichester, 2004.

(5) Espinet, P.; Echavarren, A. M. *Angew. Chem., Int. Ed.* **2004**, *43*, 4704.

(6) (a) Casado, A. L.; Espinet, P. *J. Am. Chem. Soc.* **1998**, *120*, 8978. (b) Casado, A. L.; Espinet, P. J.; Gallego, A. M. *J. Am. Chem. Soc.* **2000**, *122*, 11771. (c) Casares, J. A.; Espinet, P.; Salas, G. *Chem. Eur. J.* **2002**, *8*, 4844.

(7) Napolitano, E.; Farina, V.; Persico, M. *Organometallics* **2003**, *22*, 4030.

(8) Álvarez, R.; Faza, O. N.; López, C. S.; de Lera, Á. R. *Org. Lett.* **2006**, *8*, 35.



[Pd(Ar)(I)(P'Bu₃)] complex is slower than that of the related complex [Pd(Ar)(Br)(P'Bu₃)], an observation attributable to the strength of the Pd(II)–X bond.⁹

Clearly, a more electronegative halide, acting as a leaving ligand, accelerates the transmetalation process. In this paper, with the aid of B3LYP density functional theory (DFT) calculations, we detail investigations into model transmetalation reactions of (vinyl)SnMe₃ with (PH₃)₂Pd(Ph)(X) (X = Cl, Br, I) in order to provide a deeper insight into how the X ligands influence the transmetalation reactions of R'SnR''₃ with L_nPd(R)(X). We will also briefly discuss the effect of phosphine ligands because phosphine ligands of high donicity have been found to impede transmetalation,¹⁰ which is potentially a hindrance in the cross-coupling of stronger C–Cl bonds in the organohalide component, as an electron-rich ligand is often required for C–Cl activation. Transmetalation of (vinyl)SnMe₃ with (PMe₃)Pd(vinyl)(Br) was found to be the rate-determining step in a theoretical study on the Stille cross-coupling reaction of the vinyl bromide.⁸ Through our understanding on how the leaving ligand X affects the rate of transmetalation, we also wish to report further computational investigations to support the S_E2(cyclic) mechanism proposed by Espinet and co-workers.^{5,6}

Computational Details

Gaussian 03¹¹ was used to fully optimize all the structures reported in this paper at the B3LYP¹² level of density functional theory. Frequency calculations were carried out at the same level of theory for all the stationary points to characterize the transition states (one imaginary frequency) and the equilibrium structures (no imaginary frequency). The effective core potentials of Hay and Wadt with double- ζ valance basis sets (LanL2DZ)¹³ were chosen to describe Pd, Cl, Br, I, Sn, and P. The 6-31G¹⁴ basis set was used for other atoms. Polarization functions were also added for C($\zeta_d = 0.6$), Cl($\zeta_d = 0.514$), Br($\zeta_d = 0.389$), I($\zeta_d = 0.266$), Sn($\zeta_d = 0.183$), and P($\zeta_d = 0.340$).¹⁵ Calculations of intrinsic reaction coordinates (IRC)¹⁶ were also performed on transition states to confirm that such structures are indeed connecting two minima.

(9) See p 4712 of ref 4.

(10) (a) Farina, V.; Krishnan, B. *J. Am. Chem. Soc.* **1991**, *113*, 9585.

(b) Farina, V. *Pure Appl. Chem.* **1996**, *68*, 73.

(11) Frisch, M. J.; et al. *Gaussian 03*, revision B05; Gaussian, Inc.: Pittsburgh, PA, 2003.

(12) (a) Becke, A. D. *J. Chem. Phys.* **1993**, *98*, 5648. (b) Lee, C.; Yang, W.; Parr, R. G. *Rev. Phys. B* **1988**, *37*, 785.

(13) (a) Wadt, W. R.; Hay, P. J. *J. Chem. Phys.* **1985**, *82*, 284. (b) Hay, P. J.; Wadt, W. R. *J. Chem. Phys.* **1985**, *82*, 299.

(14) Hariharan, P. C.; Pople, J. A. *Theor. Chim. Acta* **1973**, *28*, 213.

(15) Huzinaga, S. *Gaussian Basis Sets for Molecular Calculations*; Elsevier Science Pub. Co.: Amsterdam, 1984.

(16) (a) Fukui, K. *J. Phys. Chem.* **1970**, *74*, 4161. (b) Fukui, K. *Acc. Chem. Res.* **1981**, *14*, 363.

The partial atomic charges were calculated on the basis of natural bond orbital (NBO)¹⁷ analyses.

Results and Discussion

In the majority of Stille coupling reactions, the first step involves oxidative addition of ArX to the coordinatively unsaturated 14-electron species “L₂Pd(0)”.¹⁸ We accept that some of these reactions might involve the 12-electron species “LPd(0)”, where L = a bulky phosphine or an *N*-heterocyclic carbene.¹⁹ Experimental studies,²⁰ supported by theoretical work,²¹ have suggested that ArX reacts with Pd(0) by a three-centered transition state, giving rise to a *cis*-(L)₂Pd(Ar)(X) complex. The *cis*-isomer subsequently isomerizes to the thermodynamically more stable *trans*-isomer. Thus, it is reasonable to consider the model complexes *trans*-(PH₃)₂Pd(Ph)(X) (X = Cl, Br, I) as the active species for transmetalation reactions.

A recent theoretical study⁸ provided more details regarding the mechanism of transmetalation of (vinyl)Sn(R'')₃ with *trans*-(L)₂Pd(R)(X), which consists of two key steps shown in Scheme 2: (1) formation of a π -complex **2**, from **1** through an associative substitution of one of the phosphine ligands with (vinyl)Sn(Me)₃ via transition state **TS**_{1–2}; and (2) transmetalation in the π -complex proceeding via a cyclic four-coordinate transition state **TS**_{2–3} giving **3**.

The calculated potential energy profiles for the transmetalation of *trans*-(PH₃)₂Pd(Ph)(X) (X = Cl, Br, I) on the basis of the mechanism described in Scheme 2 are shown in Figure 1. It can be seen that the transmetalation processes for the complexes, where X = Cl, Br, and I, take place with overall activation barriers of 13.7, 18.0, and 22.3 kcal/mol, respectively. These results are consistent with the experimental observations that more electronegative halide ligands accelerate transmetalation of R'SnR''₃ with L_nPd(R)(X).

Substitution of PH₃ with (vinyl)SnMe₃. Let us first discuss the ligand substitution step (**1**_X → **2**_X) in the transmetalation processes. The ligand substitution is endothermic in all cases (Figure 1). The reaction energy of the ligand substitution, i.e., the energy difference between **1**_X and (vinyl)SnMe₃ and **2**_X and PH₃, is reliant on the nature of the ligand X: 0.8 kcal/mol for X = Cl, 2.4 kcal/mol for X = Br, and 4.1 kcal/mol for X = I (Figure 1). To understand the trend established in the substitution reaction energies, we calculated the ligand dissociation energies of PH₃ in **1**_X and the π -complexation energies of (vinyl)SnMe₃ in **2**_X. The ligand dissociation energies of PH₃ in **1**_{Cl}, **1**_{Br}, and **1**_I were calculated as 22.8,

(17) Glendening, E. D.; Read, A. E.; Carpenter, J. E.; Weinhold, F. *NBO* (version 3.1); Gaussian, Inc.: Pittsburgh, PA, 2003.

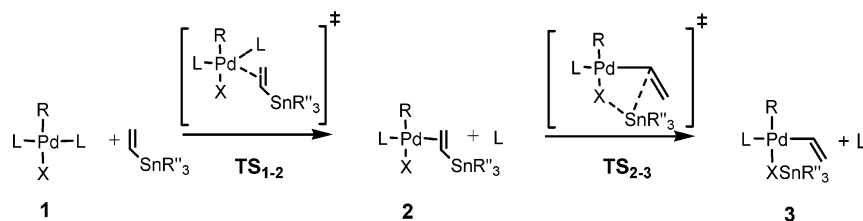
(18) (a) Meijere, A. de; Meyer, F. E. *Angew. Chem., Int. Ed. Engl.* **1994**, *33*, 2379. (b) Crisp, G. T. *Chem. Soc. Rev.* **1998**, *27*, 427. (c) Beletskaya, I. P.; Cheprakov, A. V. *Chem. Rev.* **2000**, *100*, 3009.

(19) The importance of low-ligated Pd⁰ complexes has been reviewed; see: (a) Christmann, U.; Vilar, R. *Angew. Chem., Int. Ed.* **2005**, *44*, 366. For the in situ preparation of monoligated “Ph₃P–Pd⁰”, see: (b) Beeby, A.; Bettington, S.; Fairlamb, I. J. S.; Goeta, A. E.; Kapdi, A. R.; Thompson, A. L. *New J. Chem.* **2004**, *28*, 600.

(20) (a) Urata, H.; Tanaka, M.; Fuchikami, T. *Chem. Lett.* **1987**, 751. (b) Carpentier, J.-F.; Castanet, Y.; Brocard, J.; Mortreux, A.; Rose-Munch, F.; Susanne, C.; Rose, E. *J. Organomet. Chem.* **1995**, *493*, C22. (c) Casado, A. L.; Espinet, P. *Organometallics* **1998**, *17*, 954. (d) Füstner, A.; Seidel, G.; Kremzow, D.; Lehmann, C. W. *Organometallics* **2003**, *22*, 907.

(21) (a) Sundermann, A.; Uzan, O.; Martin, J. M. L. *Chem. Eur. J.* **2001**, *7*, 1703. (b) Jakt, M.; Johannissen, L.; Rzepa, H. S.; Widdowson, D. A.; Wilhelm, A. J. *Chem. Soc., Perkin Trans. 2* **2002**, 576. (c) Goossen, L. J.; Koley, D.; Hermann, H. L.; Thiel, W. *Chem. Commun.* **2004**, 2141. (d) Goossen, L. J.; Koley, D.; Hermann, H. L.; Thiel, W. *Organometallics* **2005**, *24*, 2398. (e) Kozuch, S.; Amatore, C.; Jutand, A.; Shaik, S. *Organometallics* **2005**, *24*, 2319. (f) Senn, H. M.; Ziegler, T. *Organometallics* **2004**, *23*, 2980. (g) Ariafard, A.; Lin, Z. *Organometallics* **2006**, *25*, 4030.

Scheme 2



22.8, and 23.0 kcal/mol, respectively. The trend found in the ligand dissociation energies of PH_3 suggests that the influence of the X ligands on the dissociation energies is negligible. In contrast, the π -complexation of $(\text{vinyl})\text{SnMe}_3$ becomes more favorable along the series $\text{X} = \text{I} < \text{Br} < \text{Cl}$ (-18.9 kcal/mol for **2_I**, -20.3 kcal/mol for **2_Br**, and -21.9 kcal/mol for **2_Cl**). The observed trend in the π -complexation energies can be rationalized through consideration of the steric repulsion between the X and $(\text{vinyl})\text{SnMe}_3$ ligands; the larger the halide ligand X in size, the stronger the repulsive interaction and the smaller the π -complexation energy.

To further support the steric argument above, we calculated the π -complexation energy for the model complexes $(\text{PH}_3)_2(\text{ethylene})\text{Pd}(\text{Ph})(\text{X})$ in which the $(\text{vinyl})\text{SnMe}_3$ ligand of $(\text{PH}_3)_2$

$(\text{vinyl})\text{SnMe}_3\text{Pd}(\text{Ph})(\text{X})$ is replaced by ethylene. The calculated π -complexation energies of ethylene in $(\text{PH}_3)_2(\text{ethylene})\text{Pd}(\text{Ph})(\text{X})$ follow the same trend, -18.9 kcal/mol for $\text{X} = \text{I}$, -19.6 kcal/mol for $\text{X} = \text{Br}$, and -20.1 kcal/mol for $\text{X} = \text{Cl}$. However, the halide dependence of the π -complexation energies of ethylene is smaller than that of $(\text{vinyl})\text{SnMe}_3$ because the ethylene ligand is sterically less demanding than $(\text{vinyl})\text{SnMe}_3$. We also examined the effect of the X ligands on the P–Pd–X angles (Scheme 3). We can see from Scheme 3 that the reduction in the P–Pd–I angle from the $(\text{PH}_3)_2\text{Pd}(\text{Ph})(\text{I})$ metal fragments to the olefin-coordinated complex $(\text{PH}_3)_2\text{Pd}(\text{Ph})(\text{I})(\eta^2\text{-olefin})$ is the largest, 33.2° for olefin = $(\text{vinyl})\text{SnMe}_3$ and 32.0° for olefin = ethylene. The reduction is the smallest when $\text{X} = \text{Cl}$, 30.2° for both olefins. All these results are consistent with the steric argument.

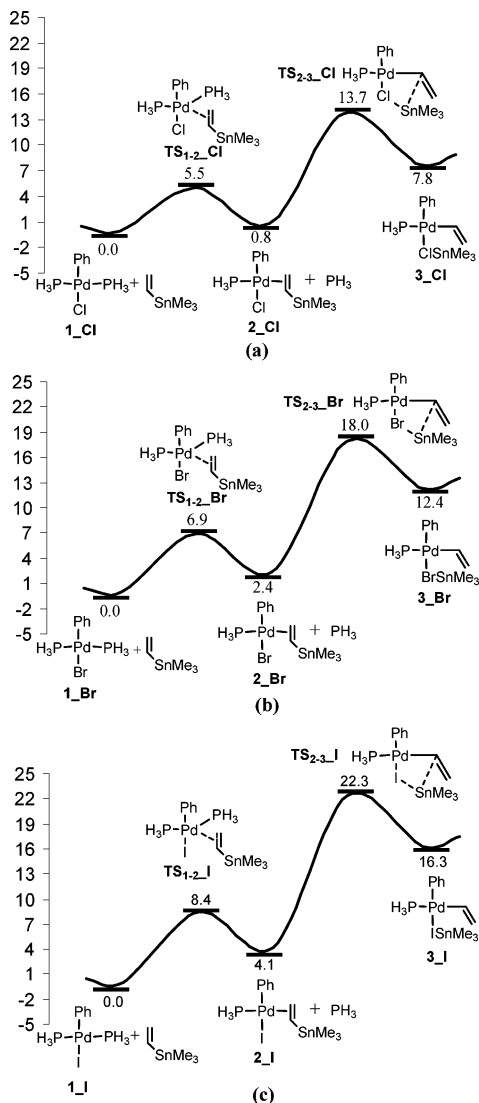
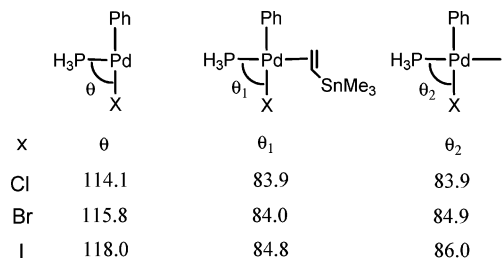


Figure 1. Potential energy profiles calculated for the transmetalation of $\text{trans}-(\text{PH}_3)_2\text{Pd}(\text{Ph})(\text{X})$ ($\text{X} = \text{Cl}, \text{Br}, \text{I}$) with $(\text{vinyl})\text{SnMe}_3$ on the basis of the mechanism described in Scheme 2.

Scheme 3



One may ask whether or not the observed trend in the π -complexation energies of $(\text{vinyl})\text{SnMe}_3$ can be explained through electronic reasoning. It has been established that the dominating bonding interaction between an η^2 -olefin and a Pd(II) metal center is the olefin(π)-to-Pd(II) σ -donation.²² The C–C double-bond distances of the η^2 -coordinated $(\text{vinyl})\text{SnMe}_3$ were calculated as 1.376 \AA for all three **2_X** complexes (Figure 2), indicating that the Pd(d)-to-olefin(π^*) back-donation is approximately the same regardless what X is. Because of the dominant olefin(π)-to-Pd(II) σ -donation, we expect a good correlation between the π -complexation energies and the total partial charges on the coordinated olefin ligand.^{22c} The total Mulliken and NBO partial charges on the coordinated $(\text{vinyl})\text{SnMe}_3$ ligand in complexes **2_X** are given in Table 1. Despite the noticeable small differences, we can still see that the total partial charge on the coordinated $(\text{vinyl})\text{SnMe}_3$ ligand gradually increases on going from **2_Cl** to **2_I**, indicating that the coordinated $(\text{vinyl})\text{SnMe}_3$ ligand donates more electrons to the $(\text{PH}_3)_2\text{Pd}(\text{Ph})(\text{X})$ metal fragment when $\text{X} = \text{I}$ than when $\text{X} = \text{Br}$ and $\text{X} = \text{Cl}$. In other words, the $(\text{PH}_3)_2\text{Pd}(\text{Ph})(\text{X})$ metal fragment gains more electrons from the coordinated $(\text{vinyl})\text{SnMe}_3$ ligand when $\text{X} = \text{I}$. As mentioned above, the π -complexation of $(\text{vinyl})\text{SnMe}_3$ becomes more favorable along the series $\text{X} = \text{I} < \text{Br} < \text{Cl}$ (-18.9 kcal/mol for **2_I**, -20.3 kcal/mol for **2_Br**, and -21.9 kcal/mol for **2_Cl**), suggesting that

(22) (a) Stromberg, S.; Svensson, M.; Zetterberg, K. *Organometallics* **1997**, *16*, 3165. (b) Szabo, M. J.; Jordan, R. F.; Michalak, A.; Piers, W. E.; Weiss, T.; Yang, S.-Y.; Ziegler, T. *Organometallics* **2004**, *23*, 5565. (c) Zhao, H.; Ariafard, A.; Lin, Z. *Inorg. Chim. Acta* **2006**, *359*, 3527.

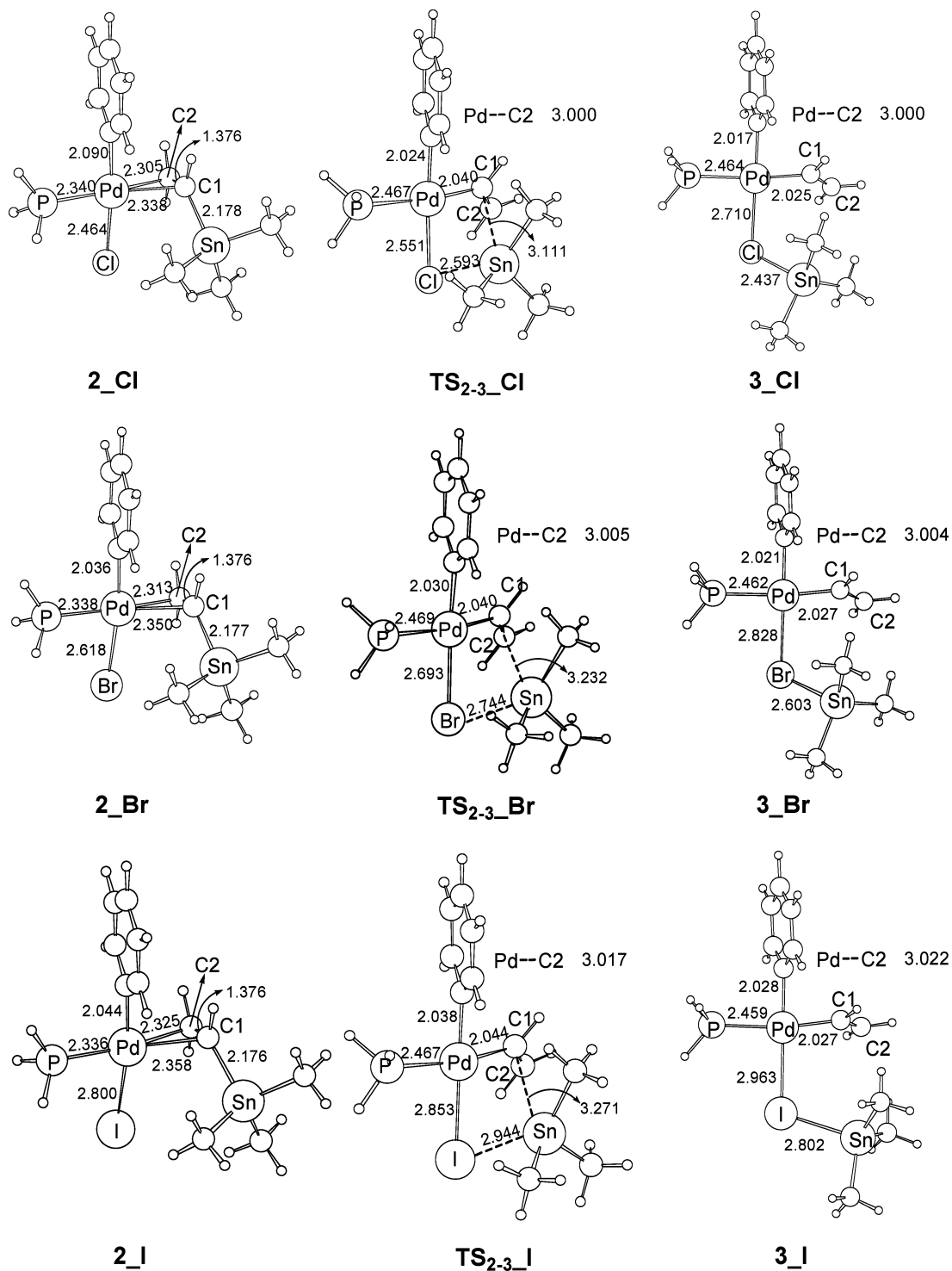


Figure 2. Calculated structures for species involved in the transmetalation step of *trans*-(PH_3) $_2$ Pd(Ph)(X) (X = Cl, Br, I) with (vinyl)- SnMe_3 .

Table 1. NBO and Mulliken Partial Charges on the (vinyl) SnMe_3 Ligand in 2_Cl, 2_Br, and 2_I

partial charges of (vinyl) SnMe_3	2_Cl	2_Br	2_I
NBO	+0.113	+0.115	+0.117
Mulliken	+0.286	+0.297	+0.305

gaining more electrons from the coordinated olefin does not lead to a greater π -complexation energy. Therefore, the observed trend in the π -complexation energies cannot be explained by electronics alone and that the proposed steric argument is justified. The result that the $(\text{PH}_3)\text{Pd}(\text{Ph})(\text{X})$ metal fragment,

when X = I, gains more electrons from the coordinated olefin than when X = Cl is quite unexpected because one would feel that the metal center should carry more positive charge when X = Cl and in turn gain more electron transfer from the coordinated olefin ligand. The unexpected result can be understood by invoking the π -donation properties of chloride. The Pd(II)–(vinyl) SnMe_3 interaction is dominated by donation from the π -bonding orbital of (vinyl) SnMe_3 to the Pd(II) center. The LUMO of the $(\text{PH}_3)\text{Pd}(\text{Ph})(\text{X})$ metal fragment, responsible for accepting electrons from the coordinated olefin ligand, is $d_{x^2-y^2}$, which is slightly σ^* -antibonding with both the Ph and

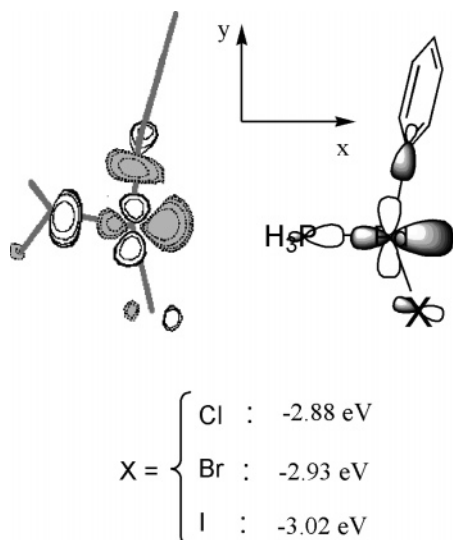


Figure 3. LUMO of the $(\text{PH}_3)\text{Pd}(\text{Ph})(\text{X})$ ($\text{X} = \text{Cl}, \text{Br}, \text{I}$) metal fragment that is responsible for accepting electrons from the coordinated olefin ligand.

PH_3 ligands' hybrid orbitals and slightly π^* -antibonding with the X ligand's p_π orbital (Figure 3). The slightly π^* -antibonding interaction is more significant when X is Cl because the Pd–Cl bond is the shortest among the three Pd–X bonds. Figure 3 shows that the LUMO energy decreases from -2.88 eV for $(\text{PH}_3)\text{Pd}(\text{Ph})(\text{Cl})$ to -2.93 eV for $(\text{PH}_3)\text{Pd}(\text{Ph})(\text{Br})$ and then to -3.02 eV for $(\text{PH}_3)\text{Pd}(\text{Ph})(\text{I})$. The $(\text{PH}_3)\text{Pd}(\text{Ph})(\text{I})$ metal fragment has the lowest LUMO orbital, and therefore, the electron transfer from the coordinated ligand to the metal fragment is the most significant.

1_X undergoes dissociation of one of the PH_3 ligands by substitution with $(\text{vinyl})\text{SnMe}_3$ via the transition state TS_{1-2_X} , giving 2_X . The transition state TS_{1-2_X} adopts a typical trigonal-bipyramidal structure with the Ph and X ligands occupying the two axial sites. The reaction barriers of $1_X \rightarrow 2_X$ are closely related to the stability of 2_X . The barriers increase down the group and range from 5.5 kcal/mol for $\text{X} = \text{Cl}$ to 8.4 kcal/mol for $\text{X} = \text{I}$ (Figure 1).

Transmetalation. The transmetalation step corresponds to the transfer of the SnMe_3 group from the coordinated $(\text{vinyl})\text{SnMe}_3$ to the X ligand via a four-membered ring transition state TS_{2-3_X} , leading to the formation of 3_X (Figure 1). Here we used SnMe_3 to model SnBu_3 commonly used in experiments. In view of the calculated transition state structures shown in Figure 2, we do not expect that the steric bulk of the SnR_3 affects the qualitative conclusions we are going to make here. The $2_X \rightarrow 3_X$ conversion is endothermic in all the cases. It can be seen from Figure 1 that more electronegative halide ligands make the transmetalation step more favorable both kinetically and thermodynamically. The barrier from 2_X is as follows: 12.9, 15.6, and 18.2 kcal/mol for $\text{X} = \text{Cl}, \text{Br},$ and I , respectively. The stability of 3_X relative to 2_X is as follows: 7.0, 10.0, and 12.2 kcal/mol for $\text{X} = \text{Cl}, \text{Br},$ and I , respectively.

Structural parameters of 2_X , 3_X , and TS_{2-3_X} are summarized in Figure 2. In each transition state structure, the Sn–X bond is almost formed, while the Sn–C(1) bond is almost cleaved. Upon going from 2_X to TS_{2-3_X} , a reorganization happens in the vinyl group; the Pd–C(1) bond is shortened, while the Pd–C(2) bond is lengthened. The Pd–C(1) and Pd–C(2) bond distances in TS_{2-3_X} are almost the same as those in 3_X . From these results, we concluded that these transition states are quite product-like. Thus, the stabilities of the transition

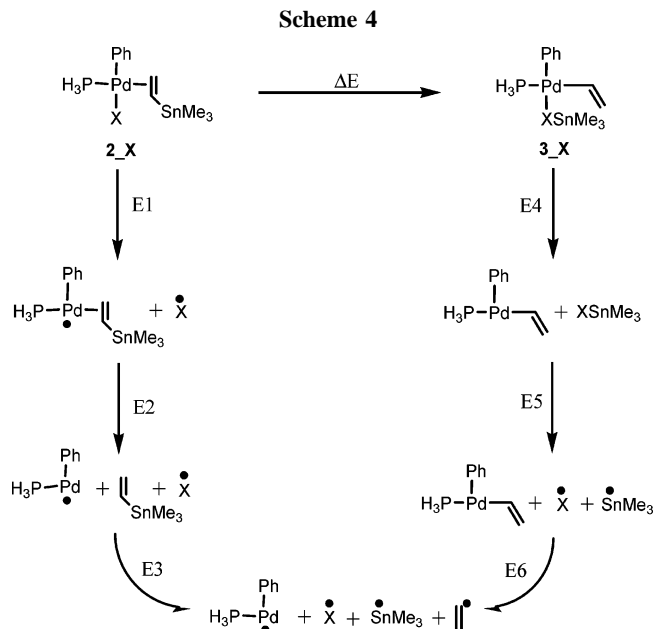


Table 2. Bond Energies (kcal/mol) Calculated for the Pd–X ($E1$), Pd–(XSnMe_3) ($E4$), and X– SnMe_3 ($E5$) Bonds

X	$E1$	$E4$	$E5$	$E1 - E4 - E5$
Cl	78.5	8.6	97.5	–27.6
Br	68.1	8.0	84.8	–24.7
I	58.8	7.6	73.6	–22.4

states TS_{2-3_Cl} , TS_{2-3_Br} , and TS_{2-3_I} correlate well with those of 3_Cl , 3_Br , and 3_I , respectively.

To understand the trend observed in the endothermicity in the conversion of $2_X \rightarrow 3_X$, the reaction energies for the conversion based on a hypothetical energy decomposition analysis shown in Scheme 4 were calculated. According to this analysis, the reaction energy (ΔE) for a given $2_X \rightarrow 3_X$ conversion can be described in eq 1.

$$\Delta E = E1 + E2 + E3 - E4 - E5 - E6 \quad (1)$$

$E1$ represents the Pd–X homolytic bond dissociation energy in 2_X , where geometries $(\text{PH}_3)(\text{Ph})(\text{vinylSnMe}_3)\text{Pd}^*$ and X^* are fully optimized. $E2$ is the energy required to dissociate the $(\text{vinyl})\text{SnMe}_3$ ligand from $(\text{PH}_3)(\text{Ph})(\text{vinylSnMe}_3)\text{Pd}^*$ to give $(\text{PH}_3)(\text{Ph})\text{Pd}^*$. The vinyl– SnMe_3 homolytic bond dissociation energy ($E3$) was evaluated by calculating the energy difference between $(\text{vinyl})\text{SnMe}_3$ and the energy sum of the optimized fragments vinyl^* and $^*\text{SnMe}_3$. $E4$ is the bond energy derived from the X-to-metal dative bonding interaction in 3_X . $E5$ represents the homolytic bond dissociation energy of the Sn–X bond, and $E6$ refers to the energy needed to homolytically cleave the Pd–C bond in $(\text{PH}_3)(\text{Ph})\text{Pd}(\text{vinyl})$ to form $(\text{PH}_3)(\text{Ph})\text{Pd}^*$ and vinyl^* . Equation 1 can be further simplified to eq 2 because the $E2$, $E3$, and $E6$ terms are independent of X.

$$\Delta E = E1 - E4 - E5 + \text{constant} \quad (2)$$

The calculated values of $E1$, $E4$, $E5$, and $E1 - E4 - E5$ are given in Table 2. It follows that the Pd–X and Sn–X homolytic bond dissociation energies, $E1$ and $E5$, respectively, increase in the order $\text{X} = \text{I} < \text{Br} < \text{Cl}$. This trend is in agreement with the general rule that the A–X homolytic bond dissociation energies increase with decreasing size and increasing electro-

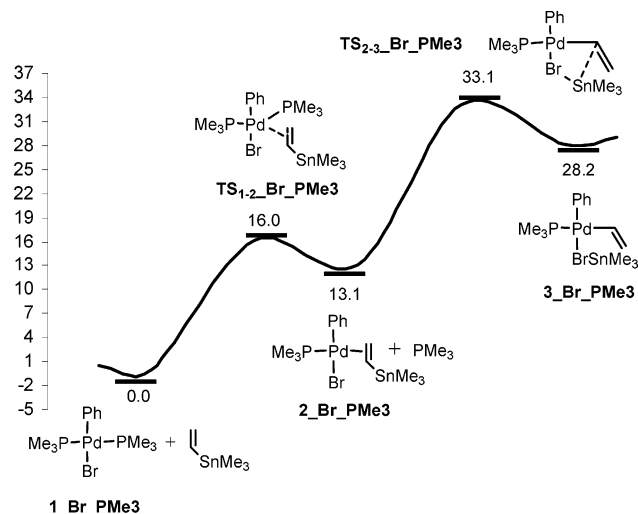


Figure 4. Potential energy profile calculated for the model transmetalation reaction of *trans*-(PMe₃)₂PdPh(Br) with (vinyl)SnMe₃.

negativity of X.²³ The X-to-Pd dative bonding energy (*E*₄) in **3**_X also increases in the order X = I < Br < Cl, but the variation is not significant. Therefore, that the *E*₁ – *E*₄ – *E*₅ values become more negative from –22.4 for X = I to –27.6 kcal/mol for X = Cl is a result of the Sn–X bond energies (*E*₅) increasing faster than the Pd–X bond energies (*E*₁) in the order X = I < Br < Cl.

Effect of Phosphine Ligands. As mentioned in the Introduction, phosphine ligands of high donicity impede transmetalation, although bulky ligands are expected to assist this process.¹⁰ To assess the effect, we studied the model transmetalation reaction of (vinyl)SnMe₃ with *trans*-(PMe₃)₂PdPh(Br) and compared the results with those from the model reaction of (vinyl)SnMe₃ with *trans*-(PH₃)₂PdPh(Br). Figure 4 shows the energy profile calculated for the model reaction, and Figure 5 shows the calculated structures for the species involved in the reaction. The energy profile resembles those shown in Figure 1. The calculated structures are comparable with those shown in Figure 2. However, we can see that the overall barrier for the transmetalation process of the PMe₃ system (Figure 4) is significantly higher than that of the corresponding PH₃ system (Figure 1b), 33.1 versus 18.0 kcal/mol, consistent with the experimental observation that phosphine ligands of high donicity impede transmetalation.¹⁰

Carefully checking Figure 1b against Figure 4, we found that both the (vinyl)SnMe₃-for-phosphine substitution step and the transmetalation step contribute to the significant increase (by 15.1 kcal/mol) in the overall barrier from the PH₃ system to the PMe₃ system. **1**_{Br} → **2**_{Br} is endothermic by only 2.4 kcal/mol (Figure 1b). However, **1**_{Br}PMe₃ → **2**_{Br}PMe₃ is endothermic by 13.1 kcal/mol. On the basis of these results, we can say that the (vinyl)SnMe₃-for-phosphine substitution step contributes 10.7 kcal/mol to the total increase of 15.1 kcal/mol in the overall barrier from the PH₃ system to the PMe₃ system, while the transmetalation step contributes only 4.4 kcal/mol. In the (vinyl)SnMe₃-for-phosphine substitution step, *trans*-(PR₃)₂PdPh(Br) + (vinyl)SnMe₃ → (PR₃)₂(η²-vinyl)SnMe₃PdPh(Br) + PR₃, PMe₃ gives greater endothermicity than PH₃. The dissociation energy of PMe₃ in **1**_{Br}PMe₃ (30.8 kcal/mol) is calculated to be greater than that of PH₃ in **1**_{Br} (22.8 kcal/

mol). The result suggests that the two Pd–PMe₃ bonds in a *trans* arrangement do not significantly weaken each other, although PMe₃ is a stronger *trans* influence ligand than PH₃. Clearly, the stronger Pd–PMe₃ bond, as a result of PMe₃ being a better donor than PH₃,²⁴ contributes to the greater endothermicity. In addition, as the PMe₃ ligand is sterically more demanding and electronically stronger *trans*-influencing than PH₃, the Pd(II)–(η²-vinyl)SnMe₃ bonding interaction is weakened when PMe₃ is present. The Pd–C bond distances in the Pd(II)–(η²-vinyl)SnMe₃ structural unit of **2**_{Br}PMe₃ (Figure 5) are indeed longer than those of **2**_{Br} (Figure 2).

The barrier difference in the transmetalation step between the two (PH₃ and PMe₃) systems correlates well with their endothermicity difference. The greater endothermicity of **2**_{Br}PMe₃ → **3**_{Br}PMe₃ versus **2**_{Br} → **3**_{Br} can be again explained by the stronger *trans*-influencing property of PMe₃ versus PH₃. In **3**_{Br}PMe₃, both the PMe₃ and vinyl ligands are strongly *trans*-influencing and their *trans* arrangement is destabilizing. Indeed, we can see that the Pd–C bond distance in **3**_{Br}PMe₃ (Figure 5) is longer than that in **3**_{Br} (Figure 2).

In this subsection, we have demonstrated that the more electron-donating phosphine PMe₃ significantly increases the overall transmetalation barriers. Here, one may question the validity of the conclusions made in the preceding subsections due to the use of PH₃ as the model phosphine ligand. It should be noted that the conclusions made in the preceding subsections focus on the comparison of different leaving ligands X. Regardless what phosphine ligands were used, the conclusions should be valid.

Conclusion

The effect of the leaving ligand X on the transmetalation of (vinyl)SnMe₃ with *trans*-(PH₃)₂Pd(Ph)(X) (X = Cl, Br, I), commonly found in Stille cross-coupling reactions, has been theoretically studied with the aid of DFT calculations at the B3LYP level. The calculations show that the overall activation barrier for the transmetalation process, substitution of one of the PH₃ ligands with (vinyl)SnMe₃ followed by transmetalation, increases in the order X = Cl < Br < I. The results are consistent with experimental observation that a more electronegative leaving ligand assists the transmetalation process. Our analysis shows that the energetics associated with the transmetalation of *trans*-L(η²-vinyl)SnMe₃Pd(Ar)(X) → *trans*-L(η¹-vinyl)Pd(Ar)(XSnMe₃) are closely related to the Pd–X and Sn–X bond energies. The trend that the transmetalation barrier decreased in the order X = I > Br > Cl is related to the fact that the Sn–X bond energy increases faster than the Pd–X bond energy in the order X = I < Br < Cl.

By employing the S_E2(cyclic) mechanism proposed by Espinet and co-workers, we have shown that it is possible to theoretically reproduce and explain the trend observed experimentally, thus further validating their proposal. Finally, it should be emphasized that for aryl chlorides, although the transmetalation step is faster than for aryl iodides, the oxidative addition step is rate-determining and difficult, making the corresponding Stille cross-coupling reactions much more challenging.²⁵

More electron-donating phosphine ligands were found to significantly increase the overall transmetalation barriers. A more electron-donating phosphine ligand gives a stronger Pd–P

(23) (a) Sakaki, S.; Biswas, B.; Musashi, Y.; Sugimoto, M. *J. Organomet. Chem.* **2000**, *611*, 288. (b) Rauk, A. *Orbital Interaction Theory of Organic Chemistry*; Wiley-Interscience: New York, 2001.

(24) Niu, S.; Hall, M. B. *Chem. Rev.* **2000**, *100*, 353.

(25) (a) Littke, A. F.; Fu, G. C. *Angew. Chem., Int. Ed.* **1999**, *38*, 2411. (b) Littke, A. F.; Schwarz, L.; Fu, G. C. *J. Am. Chem. Soc.* **2002**, *124*, 6343.

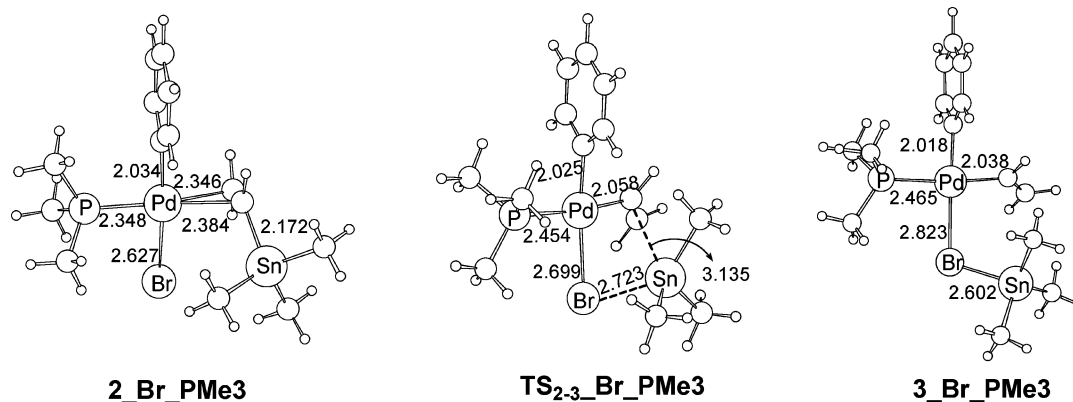


Figure 5. Calculated structures for species involved in the model transmetalation reaction of *trans*-(PMe₃)₂PdPh(Br) with (vinyl)SnMe₃.

bond, making the substitution of phosphine with (vinyl)SnR₃ difficult. At the same time, it exerts a stronger *trans* influence on the Pd–vinyl bond, destabilizing the transmetalation product.

Acknowledgment. We acknowledge financial support from the Hong Kong Research Grants Council (Grant Nos. HKUST 6023/04P and DAG05/06.SC19), and I.J.S.F. thanks the Royal Society for a research fellowship and EPSRC for funding related aspects of this research (Grant No. EP/D078776/1). A.A.

appreciates the financial support from Islamic Azad University, Iran.

Supporting Information Available: Complete ref 11 and tables giving Cartesian coordinates and electronic energies for all the calculated structures. This material is available free of charge via the Internet at <http://pubs.acs.org>.

OM0607705